Sensitive frequency dependence of the carrier-envelope phase effect on bound-bound transitions: An interference perspective

Dian Peng (彭典),[1] Biao Wu (吴飙),[2,3] Panming Fu (傅盘铭),[1] Bingbing Wang (王兵兵),[1,*] Jiangbin Gong (龚江滨),[4] and Zong-Chao Yan (严宗朝)[5]

[1]*Laboratory of Optical Physics, Beijing National Laboratory for Condensed Matter Physics, Institute of Physics, Chinese Academy of Sciences, Beijing 100190, China*

[2]*International Center for Quantum Materials, Peking University, Beijing 100871, China*

[3]*Department of Physics, State Key Laboratory for Artificial Microstructures and Mesoscopic Physics, Peking University, Beijing 100871, China*

[4]*Department of Physics and Center of Computational Science and Engineering, National University of Singapore, Singapore 117542, Singapore*

[5]*Department of Physics, University of New Brunswick, P.O. Box 4400, Fredericton, New Brunswick, Canada E3B 5A3*

(Received 25 September 2010; published 8 November 2010)

We investigate numerically with Hylleraas coordinates the frequency dependence of the carrier-envelope phase (CEP) effect on bound-bound transitions of helium induced by an ultrashort laser pulse of a few cycles. We find that the CEP effect is very sensitive to the carrier frequency of the laser pulse, occurring regularly even at far-off-resonance frequencies. By analyzing a two-level model, we find that the CEP effect can be attributed to the quantum interference between neighboring multiphoton transition pathways, which is made possible by the broadened spectrum of the ultrashort laser pulse. A general picture is developed along this line to understand the sensitivity of the CEP effect to the laser's carrier frequency. Multilevel influence on the CEP effect is also discussed.

DOI: 10.1103/PhysRevA.82.053407 PACS number(s): 32.80.Rm, 42.50.Hz, 32.80.Qk

I. INTRODUCTION

For an ultrashort laser pulse that lasts for only a few cycles, its carrier-envelope phase (CEP) can dramatically affect the yield of matter-laser interaction [1], leading to CEP dependence of electron ionization [2–6] and harmonic-photon emission [7–10]. Recently, with the rapid development of laser technology, CEP has become a new way to control the dynamic process of matter-laser interaction [9]. It has been demonstrated that the CEP effect for an intense laser pulse can be measured by comparing the photoelectron yields in two opposite directions along the laser's electric field [2].

More recently, the CEP effect on the bound-bound transition of an atom has been investigated theoretically [11–13] and observed experimentally [14]. Roudnev and Esry [13] have presented a general framework for understanding the CEP effect using the Floquet theory. Li *et al.* [14] have demonstrated that an experimentally observed CEP effect can be attributed to the interference between one- and three-photon transition pathways. The study by Nakajima and Watanabe [11] suggests that the CEP effect can occur as the laser's carrier frequency is far off-resonance.

In this article, we use Hylleraas coordinates to study numerically how the CEP effect on bound-bound transitions of helium changes as a function of the carrier frequency of an ultrashort laser. Our numerical results show that the CEP effect depends sensitively on the carrier frequency even when it is far off-resonance. The essential physics implied in these numerical results can be well revealed by a two-level model. For a two-level system, when the pulse duration is long, quantum transitions peak at well-separated multiphoton-resonant frequencies. As the pulse duration decreases to less than three laser cycles, for example, the widths of such transition peaks get significantly broadened, and eventually, two broadened neighboring transition peaks can cross with each other. As a result, two different multiphoton transitions can both contribute significantly to the total transition amplitude and hence interfere with each other. We show that a large CEP effect occurs exactly at these crossings and can hence be understood as a quantum interference effect [15]. A general and simple picture developed along this line enables us to clearly answer the following questions: (1) Why is the CEP effect on bound-bound transitions sensitive to a carrier frequency that is far off-resonance? (2) Which multiphoton transition pathways can interfere and lead to the CEP effect?

II. NUMERICAL METHOD TOWARD THE CEP EFFECT IN HELIUM

Atomic units are used throughout the article, unless specified otherwise. To study a photoexcitation process of a ground-state helium atom in a linearly polarized ultrashort laser pulse, we solve a time-dependent Schrödinger equation $i(\partial/\partial t)|\Psi(t)\rangle = [\mathbf{H}_0 + \mathbf{H}_1(t)]|\Psi(t)\rangle$. The field-free part of the Hamiltonian reads

$$\mathbf{H}_0 = -\frac{1}{2}\nabla_1^2 - \frac{1}{2}\nabla_2^2 - \frac{2}{r_1} - \frac{2}{r_2} + \frac{1}{|\mathbf{r}_1 - \mathbf{r}_2|}, \tag{1}$$

where $\mathbf{r}_1$ and $\mathbf{r}_2$ are the coordinates of the two electrons measured from the nucleus located at the origin. The light-atom interaction part of the Hamiltonian is

$$\mathbf{H}_1 = (\mathbf{r}_1 + \mathbf{r}_2)\cdot\mathbf{e}(t) = -(\mathbf{r}_1 + \mathbf{r}_2)\cdot\partial\mathbf{A}(t)/\partial t, \tag{2}$$

where the vector potential of the field is given by [4,16]

$$\mathbf{A}(t) = \hat{\varepsilon} A_0 \exp(-\alpha^2 t^2)\sin(\omega t + \phi)/\omega, \tag{3}$$

*wbb@aphy.iphy.ac.cn

with $\hat{\varepsilon}$ being the linear polarization vector, ω the carrier frequency, and ϕ the CEP parameter. The full width at half maximum (FWHM) of the pulse duration is $\tau = 2\sqrt{\ln 2}/\alpha$.

The wave function of helium $|\Psi(t)\rangle$ is expanded in terms of the field-free eigenvectors $|\psi_n\rangle$: $|\Psi(t)\rangle = \sum_n a_n(t)e^{-iE_n t}|\psi_n\rangle$, where $\mathbf{H}_0|\psi_n\rangle = E_n|\psi_n\rangle$. Then we numerically solve the following set of equations for the amplitudes $a_n(t)$:

$$i\frac{d}{dt}a_n(t) = \sum_m a_m(t)e^{-iE_{mn}t}H^I_{nm}(t), \tag{4}$$

where $E_{mn} = E_m - E_n$ and $H^I_{nm}(t) = \langle\psi_n|\mathbf{H}_1|\psi_m\rangle$. Initially, the helium is in the ground state. The basis set is constructed in Hylleraas coordinates [17]:

$$|\psi_n\rangle = \sum_m c_{nm}|\phi_m\rangle,$$

where

$$|\phi_m\rangle = r_1^i r_2^j r_{12}^k e^{-\alpha r_1 - \beta r_2}\mathcal{Y}^{LM}_{l_1 l_2}(\mathbf{r}_1,\mathbf{r}_2).$$

In the preceding, $\mathcal{Y}^{LM}_{l_1 l_2}(\mathbf{r}_1,\mathbf{r}_2)$ is the vector-coupled product of spherical harmonics for the two electrons. In order to obtain convergent results, 874 Hylleraas functions are used with the total angular momentum quantum number L ranging from 0 to 4.

Our numerical results show that the population of an excited state of helium can strongly depend on the CEP parameter ϕ at certain carrier frequencies. To quantify this CEP effect, we introduce the parameter [11]

$$\mathcal{M} = \frac{P(\phi_{\max}) - P(\phi_{\min})}{[P(\phi_{\max}) + P(\phi_{\min})]/2}, \tag{5}$$

where $P(\phi_{\max})$ and $P(\phi_{\min})$ are, respectively, the maximum and minimum populations for a given excited state. A large value of $\mathcal{M}$ means a strong CEP effect. We numerically calculate $\mathcal{M}$ for the $2\,^1P$ and $3\,^1D$ states. In our computation, the FWHM pulse duration is one laser cycle, and the peak intensity of the laser is 10^{13} W/cm^2.

Figure 1 presents how $\mathcal{M}$ changes with the laser carrier frequency ω. Results for the $2\,^1P$ state (squares) are shown in Fig. 1(a) and those for the $3\,^1D$ state (circles) are shown in Fig. 1(b). It is clear from the figure that there are many carrier frequency windows in which $\mathcal{M}$ peaks at about its maximum value of 2, indicating a strong CEP effect on the transition probabilities from the ground state to the two excited states. These numerical details qualitatively agree with those reported in Ref. [14], where the authors changed the energy difference between two bound states instead.

One important feature in Fig. 1 is that the CEP effect is very sensitive to the carrier frequency, even it is far off-resonance as compared with the energy difference between the two bound states. This implies that far off-resonance is not a sufficient condition for a large CEP effect. In the following, we attempt to answer the following question: What is the physics underlying these narrow frequency windows where the parameter $\mathcal{M}$ peaks?

We have compared our full numerical results in Fig. 1(a) to the results of a two-level model (to be elaborated later). As clearly shown in the figure, except the peak positions that are shifted toward lower frequencies, the two-level results

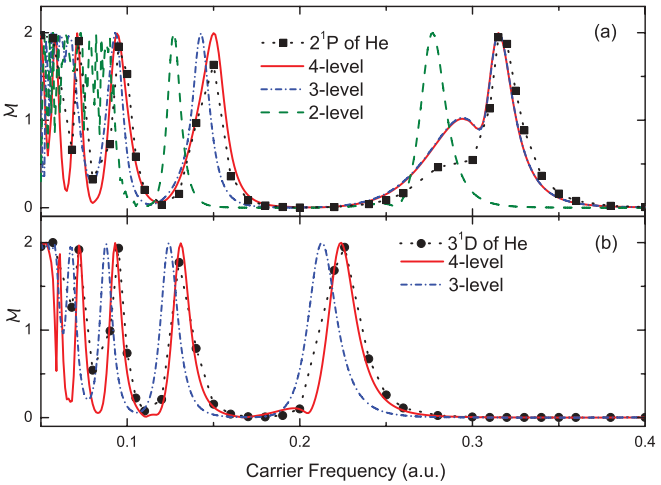

FIG. 1. (Color online) The CEP parameter $\mathcal{M}$ [see Eq. (5)] vs the laser's carrier frequency for (a) the $2\,^1P$ state and (b) the $3\,^1D$ state of helium. Solid squares and solid circles are numerical results, the (green) dashed line is for a two-level model, (blue) dash-dotted lines are for a three-level model, and (red) solid lines are for a four-level model.

[the (green) dashed curve in Fig. 1(a)] can embody the main features in the full numerical results for $\omega > 0.1$. This indicates that a simple two-level model is sufficient to reflect the essential physics behind these peaks. In the following, we first study a two-level model and then investigate multilevel influence on the CEP effect.

III. TWO-LEVEL MODEL AND INTERFERENCE BETWEEN NEIGHBORING TRANSITION PATHWAYS

Consider a two-level system in a pulsed laser field. The ground and the first excited states of helium are chosen as the two levels, denoted as $|0\rangle$ and $|1\rangle$. According to Eq. (4), the amplitudes of these two states obey the following equations:

$$\begin{aligned}\dot{a}_0(t) &= i\mu_{01}f_{01}a_1(t),\\ \dot{a}_1(t) &= i\mu_{10}f_{10}a_0(t),\end{aligned} \tag{6}$$

where $\mu_{jk} = \mu_{kj}$ represents the transition dipole moment between two quantum states $|j\rangle$ and $|k\rangle$ and $f_{jk}(t) \equiv e(t)\exp(i\Delta E_{jk}t)$, with $e(t)$ being the laser's electric field and ΔE_{jk} being the energy difference between $|j\rangle$ and $|k\rangle$.

If the system is initially in the ground state, a formal solution of a_1, after the laser pulse has passed, can be written as

$$\begin{aligned}a_1 &= i\mu_{01}\int_{-\infty}^{\infty}dt f_{10}(t) + (i\mu_{01})^3\int_{-\infty}^{\infty}\int_{-\infty}^{t}\int_{-\infty}^{t_1}f_{10}(t)f_{01}(t_1)\\ &\quad\times f_{10}(t_2)dtdt_1dt_2 + \cdots\\ &\equiv \sum_{n=0}^{\infty}T^{(2n+1)},\end{aligned} \tag{7}$$

where $T^{(2n+1)}$ represents the $(2n+1)$-photon quantum transition amplitude. For example, $T^{(1)}$ is for a one-photon transition amplitude and $T^{(3)}$ is for a three-photon transition amplitude.

To clearly understand the physics behind each amplitude $T^{(2n+1)}$, we first consider the limit of long pulse duration, that is, $\alpha \to 0$, which is easier to deal with. In this limit, after

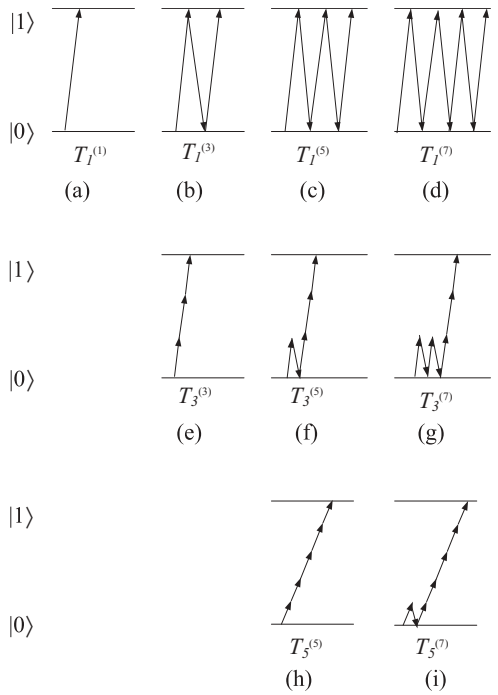

FIG. 2. Quantum transition pathways between two bound states of an atom. The pathways in the same column involve the same number of photons, e.g., the third column is for five-photon pathways. Pathways in the same row share the same resonance frequency, e.g., the pathways in the second row have the resonance frequency $\Delta E_{10}/3$, where ΔE_{10} is the energy spacing between the two bound states.

neglecting the negative frequency components [14], the $(2n+1)$-photon transition amplitude $T^{(2n+1)}$ can be decomposed into a sum of $(n+1)$ terms, that is,

$$T^{(2n+1)} \approx \sum_{j=0}^{n} T_{2j+1}^{(2n+1)}, \tag{8}$$

where

$$T_{2j+1}^{(2n+1)} \propto \delta\left[\Delta E_{10} - (2j+1)\omega\right] \exp[-i(2j+1)\phi]. \tag{9}$$

This implies that physically, each term $T_{2j+1}^{(2n+1)}$ can be associated with a quantum transition pathway, which carries a phase $-(2j+1)\phi$ and contributes significantly to the overall transition amplitude at resonant frequency $\omega_j = \Delta E_{10}/(2j+1)$. These quantum transition pathways are depicted schematically in Fig. 2, where the mth column shows all the pathways involving $(2m-1)$ photons and the kth row includes all the pathways that have a resonant frequency at $\omega_{k-1} = \Delta E_{10}/(2k-1)$, with $m \leqslant 4$ and $k \leqslant 3$.

With the decomposition in Eq. (8), it is clear that the overall transition amplitude a_1 is significantly different from zero only at resonance frequencies. At the same time, we notice that all the pathways at a given resonance frequency ω_j carry the same phase $-(2j+1)\phi$. Therefore the CEP ϕ does not affect the magnitude of a_1. This clearly explains why there is no CEP effect for a long-pulsed laser.

The situation becomes very different as the laser pulse becomes shorter. It is reasonable to assume that the decomposition in Eq. (8) still holds even for short laser pulses. However, as the pulse becomes shorter, $T_{2j+1}^{(2n+1)}$ is no longer proportional to a delta function as in Eq. (9), but becomes a function of the laser's frequency, which peaks at $\omega_j = \Delta E_{10}/(2j+1)$. Moreover, the width of the peak associated with each transition path $T_{2j+1}^{(2n+1)}$ broadens as the pulse duration gets shorter. Consequently, when the pulse is very short, for example, lasting only for a few cycles, the peaks can become so wide that the peaks for pathways $T_{2j+1}^{(2n+1)}$ with different js can cross with each other at a certain far-off-resonance frequency. As a result, the overall transition amplitude a_1 can be regarded as an interference between the two pathways if it is dominated by this pair of pathways at the crossing point. At the same time, we notice that each pathway $T_{2j+1}^{(2n+1)}$ carries the phase $-(2j+1)\phi$, indicating that the relative phase between this pair of pathways depends on the CEP ϕ. These facts mean that the overall transition amplitude a_1 depends on ϕ at the crossing point and is strongly affected by the CEP.

The preceding analysis is confirmed by our detailed numerical calculations shown in Fig. 3, where we analyze the amplitude $R = |T^{(2n+1)}|$ as a function of the laser's carrier frequency for different pulse durations while the CEP is fixed at $\phi = 0$. As clearly demonstrated in Fig. 3(a), for a laser pulse of 20 cycles, the peaks at resonance frequencies ω_0, ω_1, and ω_2 are narrow and well separated. Particularly, consistent with the preceding picture for the long pulse limit, one finds that the magnitude of $T^{(1)}$ has one peak located at ω_0, indicating the contribution from $T_1^{(1)}$, whereas the magnitude of $T^{(3)}$ has two peaks located at ω_0 and ω_1, indicating the respective contributions from $T_1^{(3)}$ and $T_3^{(3)}$. Finally the magnitude of $T^{(5)}$ has three peaks located at ω_0, ω_1, and ω_2 corresponding to $T_1^{(5)}$, $T_3^{(5)}$, and $T_5^{(5)}$, respectively. As the pulse is shortened to seven cycles, there is no essential change in the overall features, only

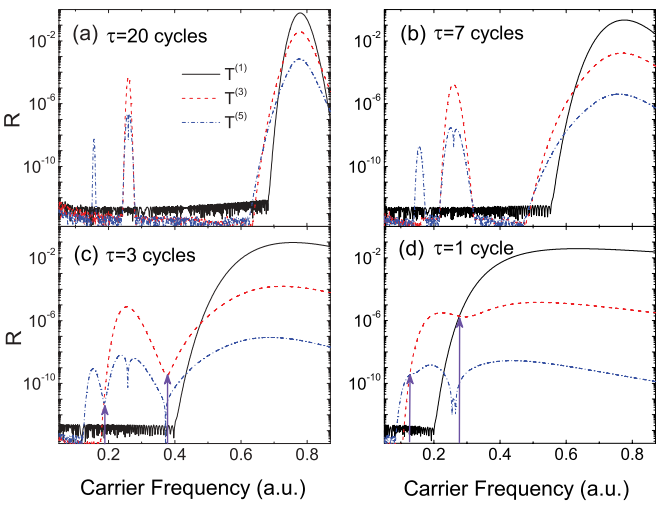

FIG. 3. (Color online) The magnitude of $T^{(2n+1)}$ with $n=0$ (solid curves), $n=1$ (dashed curves), and $n=2$ (dash-dotted curves) for pulse duration (a) $\tau = 20$, (b) $\tau = 7$, (c) $\tau = 3$, and (d) $\tau = 1$ laser cycle(s). The arrows in (c) indicate the interference between $T_3^{(3)}$ and $T_1^{(3)}$ (right) and $T_3^{(3)}$ and $T_5^{(5)}$ (left); the arrows in (d) indicate the interference between $T_1^{(1)}$ and $T_3^{(3)}$ (right) and $T_3^{(3)}$ and $T_5^{(5)}$ (left).

each peak becomes wider, as demonstrated in Fig. 3(b), which shows that the decomposition for short pulses in Eq. (8) is well justified.

It is a very different situation when the pulse is shortened to three cycles. In this case, the peaks become so broad that they begin to overlap and cross into each other. As indicated by arrows in Fig. 3(c), there are two crossings. One occurs at $\omega = 0.380$, where the peak associated with $T_1^{(3)}$ crosses with the peak associated with $T_3^{(3)}$. The other crossing happens at $\omega = 0.185$, where the peak associated with $T_3^{(3)}$ crosses with the peak associated with $T_5^{(5)}$. At such crossing points, the two dominant pathways have the same magnitude, which is essential for effective interference and strong CEP effect. Finally, when the pulse duration is decreased to one laser cycle in Fig. 3(d), the contributions from the pathways $T_1^{(1)}$ and $T_3^{(3)}$ cross with each other at $\omega = 0.277$, and the contributions from $T_3^{(3)}$ and $T_5^{(5)}$ cross at $\omega = 0.127$. Compared with the two-level results in Fig. 1, it is seen that the CEP effect occurs exactly at the frequencies where the crossings between the broadened peaks occur.

To see how the CEP affects the transition amplitude, we next investigate both the magnitudes and the phases of $T^{(1)}$, $T^{(3)}$, and $T^{(5)}$ by setting $T^{(2n+1)} = R_{T^{(2n+1)}} \exp(i\theta_{T^{(2n+1)}})$ with the pulse duration fixed at one laser cycle. The results are shown in Figs. 4(a) and 4(b) for $\phi = 0$ and Figs. 4(c) and 4(d) for $\phi = \pi/2$. Arrows in Fig. 4(a) indicate the two frequencies $\omega = 0.277$ (solid arrows) and $\omega = 0.127$ (dashed arrows) at which the CEP effect occurs. At $\omega = 0.277$, where the curves for $R_{T^{(1)}}$ and $R_{T^{(3)}}$ cross with each other, we see from Figs. 4(b) and 4(d) that the phase difference $\theta_{T^{(1)}} - \theta_{T^{(3)}}$ is around π at $\phi = 0$ and around zero at $\phi = \pi/2$. This means that when $\phi = \pi/2$, the contributions to the total transition amplitude from $T^{(1)}$ and $T^{(3)}$ constructively interfere, whereas at $\phi = 0$, they destructively interfere, leading to a significant CEP effect at $\omega = 0.277$. Therefore the CEP effect is the result of the ϕ-dependent interference between the one-photon contribution $T^{(1)}$ and the three-photon contribution $T^{(3)}$. Similarly, the strong CEP effect at $\omega = 0.127$ can be attributed to the ϕ-dependent interference between the three-photon amplitude $T^{(3)}$ and the five-photon amplitude $T^{(5)}$.

On the basis of this simple picture, it is apparent that the CEP effect often appears at a carrier frequency that is off-resonance: The contributions to the total transition amplitude from two different pathways with different js can be comparable only at a frequency that is not equal to the resonance frequency ω_j.

In principle, if the pulse duration is short enough, the transition amplitudes, which are contributed by any two neighboring pathways associated with different resonance frequencies ω_j, can interfere with each other. As such, one might expect the curve of $\mathcal{M}$ versus ω to have an infinite number of peaks. However, since the transition amplitude associated with a multiphoton pathway decreases rapidly with the number of photons involved, the actual number of clear CEP peaks will be limited by the highest order of multiphoton transitions that can have a significant transition amplitude. For example, in our two-level model with the laser intensity adopted, the highest multiphoton order is 5, thus yielding only two peaks in the curve of $\mathcal{M}$ versus ω; these two peaks arise from the interference between one- and three-photon pathways as well as between three- and five-photon pathways. If the laser intensity is further increased, then more CEP peaks can be expected. Li *et al.* [14] presented an example of the CEP effect caused by the interference between the one- and three-photon pathways, which is just one of many possible peaks in our general picture.

We next describe some computational details regarding how the laser intensity and the laser pulse duration change the CEP effect. Figure 5(a) depicts how the two CEP frequencies (i.e., the carrier frequencies at which the $\mathcal{M}$ can reach a large value) vary with the laser intensity, where the pulse duration is fixed at $\tau = 1$ laser cycle. Figure 5(b) shows the impact of the pulse duration, with the laser intensity fixed at 10^{13} W/cm^2. It is seen from Fig. 5(a) that the CEP frequency increases slightly as the intensity increases. This is because the magnitude of the multiphoton transition contribution $T^{(2n+1)}$ is proportional to $I^{(2n+1)/2}$, with I being the laser intensity. As such, the amplitudes of higher order multiphoton transitions increase with the laser intensity much faster than those of lower order ones, resulting in the crossing of neighboring peaks associated with different transition pathways occurring at higher frequencies as the laser intensity increases. Turning to the pulse duration dependence shown in Fig. 5(b), it is observed

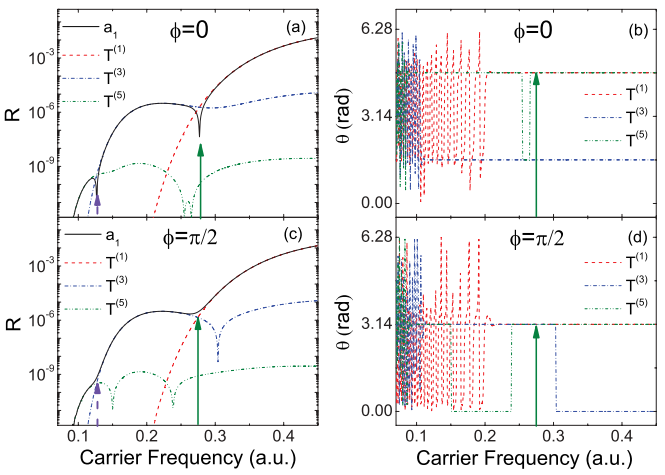

FIG. 4. (Color online) Multiphoton transition contributions to the excited state amplitudes $T^{(2n+1)}$ with $n = 0,1,2$, as a function of the laser's carrier frequency. The CEP parameter is given by (a, b) $\phi = 0$ and (c, d) $\phi = \pi/2$.

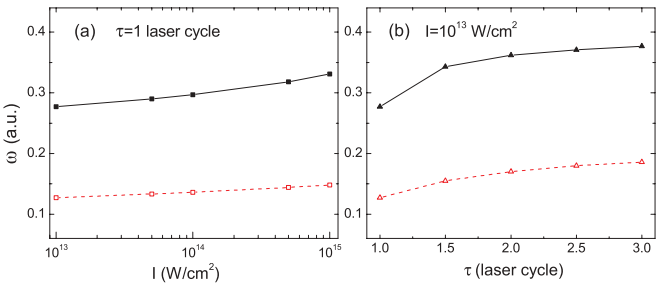

FIG. 5. (Color online) The frequency vs (a) the laser intensity and (b) the pulse duration at which the CEP effect occurs in the two-level model.

that the CEP frequencies are also slightly blue shifted as the pulse duration increases, indicating that the crossing between neighboring peaks occurs at slightly higher frequencies as the pulse duration increases. When the pulse duration is larger than about four laser cycles, the CEP effect disappears for $I = 10^{13}$ W/cm^2, implying the vanishing of crossing between any two neighboring multiphoton transition pathways.

IV. MULTILEVEL EFFECT

For a real atom, laser-atom interaction induces transitions among many states. As such, we need to consider the influence of multilevel transitions on the final population of the state of interest. As shown in Fig. 1(a), the results of the two-level model disagree quantitatively with the full numerical calculations: The two peaks at $\omega = 0.277$ and $\omega = 0.127$ appearing in the two-level model are red shifted as compared to the peaks at $\omega = 0.315$ and $\omega = 0.15$ found in the full numerical approach. One is then motivated to examine a three-level model that incorporates $|0\rangle$, $|1\rangle$, and $|2\rangle = 3\,^1D$ states of helium. Interestingly, the first peak found in this three-level model agrees well with the full numerical calculations, but the other peaks are still red-shifted as compared with those found in the full numerical calculations. Finally, we include one more level, that is, $|3\rangle = 4^1F$, in the dynamics and hence obtain a four-level model. The results from such a four-level model are found to agree well with the full numerical results for the frequency region considered here. Detailed comparisons between these models are presented in Fig. 1.

The previously mentioned quantitative differences between various models can be explained by analyzing the transition pathways in multilevel situations. Consider Eq. (7) again. Now the term $T^{(3)}$ for the three-level model includes two integrals:

$$T^{(3)} = (i\mu_{01})^3 \int_{-\infty}^{\infty}\int_{-\infty}^{t}\int_{-\infty}^{t_1} f_{10}(t) f_{01}(t_1) f_{10}(t_2)\, dt dt_1 dt_2 + (i\mu_{01})(i\mu_{12})^2 \int_{-\infty}^{\infty}\int_{-\infty}^{t}\int_{-\infty}^{t_1} f_{12}(t) f_{21}(t_1) \times f_{10}(t_2)\, dt dt_1 dt_2, \quad (10)$$

where the two integrals correspond to the following two subpaths: $|0\rangle \to |1\rangle \to |0\rangle \to |1\rangle$ (0-1-0-1) and $|0\rangle \to |1\rangle \to |2\rangle \to |1\rangle$ (0-1-2-1). Clearly both subpaths can contribute significantly to the total quantum transition amplitude from state $|0\rangle$ to state $|1\rangle$. Furthermore, the transition dipole moment μ_{12} between states $|1\rangle$ and $|2\rangle$ is larger than the transition dipole moment μ_{01} between states $|0\rangle$ and $|1\rangle$ (see Table I). This indicates that the transition amplitude from $|1\rangle$ to $|2\rangle$ is more substantial than that from $|0\rangle$ to $|1\rangle$. It can be estimated

TABLE I. Transition dipole moment of helium in atomic units. As discussed in the text, the big differences in the transition dipole moments are an important factor when explaining the quantitative differences between two-level, three-level, and four-level models.

μ_{01}	μ_{12}	μ_{23}
0.4208	2.499	5.175

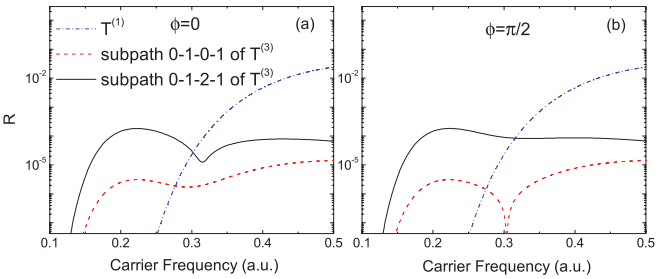

FIG. 6. (Color online) The magnitude R of $T^{(1)}$ as well as the magnitudes of the transition amplitudes formed, respectively, by the subpath 0-1-0-1 (dashed line) and by the subpath 0-1-2-1 (solid line) associated with $T^{(3)}$ as a function of the laser's carrier frequency. The results are obtained using a three-level model. In (a), the CEP parameter is given by $\phi = 0$, and in (b), the CEP parameter is given by $\phi = \pi/2$.

that the contribution by the subpath 0-1-2-1 of $T^{(3)}$ is about 1 order of magnitude larger than that by the subpath 0-1-0-1. A detailed numerical comparison between them is shown in Fig. 6. Therefore the role of the subpath 0-1-0-1 in the previous two-level model should be replaced by the subpath of 0-1-2-1 in the present three-level model, thus explaining the quantitative difference between a two-level model and a three-level model.

Similarly, for the interference between the pathways of $T^{(3)}$ and $T^{(5)}$ that accounts for the second peak at $\omega = 0.15$ in Fig. 1(a), the contribution of the subpath 0-1-2-3-2-1 to the magnitude of $T^{(5)}$ is larger than the contributions of the subpaths 0-1-2-1-2-1, 0-1-2-1-0-1, and 0-1-0-1-2-1. This can be interpreted by a four-level model. In addition, as for interference between multiphoton transitions of even higher orders, the results of the four-level model also agree well with the full numerical calculations [Fig. 1(a)]. This is because the populations of higher states are so small under the present laser conditions that the additional subpaths, including these higher states, are not important, regardless of their larger transition dipole moments.

Finally, we return to Fig. 1(b), in which $\mathcal{M}$ versus the laser's carrier frequency is shown for the $3\,^1D$ state of helium. Similar to the case of $2\,^1P$, the peaks in Fig. 1(b) can be associated with the interference between two neighboring transition paths at $\omega = \Delta E/(2n)$, where $n = 1,2,\ldots$, and ΔE is the energy spacing between the ground state and the $3\,^1D$ state. Our general picture can equally be applied to analyze this case, and the details will not be repeated here.

V. SUMMARY

In summary, we have investigated numerically the frequency dependence of the CEP effect on bound-bound transitions of helium in an ultrashort laser pulse. It has been found that the CEP effect can occur regularly even at frequencies which are far off-resonance. To explain this numerical finding, we have examined a two-level model and developed a general and simple picture, in which the total transition amplitude can be decomposed into different transition pathways. All these transition pathways can be characterized by two indices n and j, with n being the number of photons involved and j

indicating where the resonance frequency is located. For a long laser pulse, each pathway is associated with a narrow peak at the resonance frequency ω_j, and the pathways at the same resonance frequency have the same dependence on the CEP. As a result, no interference can occur between different pathways, and there is no CEP effect. In contrast, for an ultrashort pulse, the peaks for pathways at different resonance frequencies can be broadened to cross with each other. Therefore interference between different pathways can happen and lead to a strong CEP effect. This general picture is valid for a wide range of laser intensities as long as the perturbation method is applicable and can be generalized to multilevel models.

ACKNOWLEDGMENTS

This research was supported by the National Natural Science Foundation of China under Grants No. 60778009, No. 11074296, and No. 10825417 and by 973 Research Project No. 2006CB806003. Z.C.Y. was supported by NSERC of Canada and by the Canadian computing facilities ACEnet, SHARCnet, and WestGrid.

[1] F. Krausz and M. Ivanov, Rev. Mod. Phys. **81**, 163 (2009).
[2] G. G. Paulus, F. Grasbon, H. Walther, P. Villoresi, M. Nisoli, S. Stagira, E. Priori, and S. De Silvestri, Nature (London) **414**, 182 (2001).
[3] A. Baltuska *et al.*, Nature (London) **421**, 611 (2003).
[4] D. B. Milosevic, G. G. Paulus, D. Bauer, and W. Becker, J. Phys. B **39**, R203 (2006).
[5] H. Li, J. Chen, H. Jiang, P. Fu, J. Liu, Q. Gong, Z.-C. Yan, and B. Wang, Opt. Express **16**, 20562 (2008).
[6] Z. Chen, T. Wittmann, B. Horvath, and C. D. Lin, Phys. Rev. A **80**, 061402(R) (2009).
[7] A. deBohan, P. Antoine, D. B. Milosevic, and B. Piraux, Phys. Rev. Lett. **81**, 1837 (1998).
[8] A. L. Cavalieri *et al.*, New J. Phys. **9**, 242 (2007).
[9] E. Goulielmakis *et al.*, Science **320**, 1614 (2008).
[10] B. Wang, J. Chen, J. Liu, Z.-C. Yan, and P. Fu, Phys. Rev. A **78**, 023413 (2008).
[11] T. Nakajima and S. Watanabe, Phys. Rev. Lett. **96**, 213001 (2006).
[12] T. Nakajima and S. Watanabe, Opt. Lett. **31**, 1920 (2006).
[13] V. Roudnev and B. D. Esry, Phys. Rev. Lett. **99**, 220406 (2007).
[14] H. Li, V. A. Sautenkov, Y. V. Rostovtsev, M. M. Kash, P. M. Anisimov, G. R. Welch, and M. O. Scully, Phys. Rev. Lett. **104**, 103001 (2010).
[15] M. Shapiro and P. Brumer, *Principles of the Quantum Control of Molecular Processes* (Wiley, New York, 2003).
[16] S. Chelkowski and A. D. Bandrauk, Phys. Rev. A **65**, 061802(R) (2002).
[17] Z.-C. Yan and G. W. F. Drake, Chem. Phys. Lett. **259**, 96 (1996).